Chemical Doping Enhances Electronic Transport in Networks of Hexabenzocoronenes Assembled in Non-Aqueous Electrolyte

Journal:	*Polymer Chemistry*
Manuscript ID:	PY-COM-04-2015-000639.R1
Article Type:	Communication
Date Submitted by the Author:	11-Jun-2015

Complete List of Authors:	Gerber, Laura; Lawrence Berkeley National Lab, Frischmann, Peter; Lawrence Berkeley National Lab, Williams, Teresa; Lawrence Berkeley National Laboratory, The Molecular Foundry Tichelaar, Martijn; Lawrence Berkeley National Laboratory, The Molecular Foundry Tsai, Erica; Lawrence Berkeley National Laboratory, The Molecular Foundry Liu, Yi-Sheng; Lawrence Berkeley National Laboratory, Advanced Light Source Guo, Jinghua; Lawrence Berkeley National Laboratory, Pemmaraju, Chaitanya; Lawrence Berkeley National Lab, Molecular Foundry Prendergast, David; Lawrence Berkeley National Laboratory, Molecular Foundry Helms, Brett; Lawrence Berkeley National Laboratory, The Molecular Foundry

Journal Name

RSCPublishing

COMMUNICATION

Chemical Doping Enhances Electronic Transport in Networks of Hexabenzocoronenes Assembled in Non-Aqueous Electrolyte

Cite this: DOI: 10.1039/xoxxoooooox

Received ooth January 2012,
Accepted ooth January 2012

DOI: 10.1039/xoxxoooooox

www.rsc.org/

Laura C. H. Gerber,[a,b] Peter D. Frischmann,[a,b] Teresa E. Williams,[b] Martijn Tichelaar,[b] Erica Y. Tsai,[b] Yi-Sheng Liu,[c] Jinghua Guo,[c] C. D. Pemmaraju,[b] David Prendergast[b] and Brett A. Helms *[a,b]

The charge-transporting ability of supramolecular polymer networks assembled from hexabenzocoronenes (HBCs) in non-aqueous electrolyte is reported here for the first time. Enhanced electronic conductivity is observed when the HBC subunits are chemically oxidized to radical cations, which is rationalized using density functional theory.

Organic semiconductors with tunable, well-behaved charge transport have led to exciting advances for a broad range of (opto)electronic, photovoltaic and sensing technologies.[1] Recent work further highlights opportunities to integrate these materials in electrochemical devices.[2] Along these lines, we were interested in understanding their charge-transporting properties in electrolyte, toward flowable electrodes[3] with both ion and electron transport ability. Here, the electrolyte carries the ion current and the embedded organic semiconductor can be triggered, by some chemical or electrochemical means, to transport the electrons (or holes). For comparison, carbon nanomaterials with metallic or semi-metallic character confer static electronic conductivity when dispersed in electrolyte, but also improves when their loading exceeds a percolation threshold, indicating 3-D network formation is critical.[4] Notably, these nanomaterials are compositionally heterogeneous and offer limited means of tuning network conductivity and architecture through molecular engineering.[5]

We hypothesized that supramolecular polymers of polycyclic aromatic hydrocarbons[6] (PAHs) would provide an attractive platform with modular tunability (Fig. 1). Achieving success in this regard would depend on the ability of these materials to assemble into nanowires and networks in electrolyte and, furthermore, be induced to transport charge (e.g., via a hopping mechanism[7]).

Here, we show that a new hexa-*peri*-hexabenzocoronene (HBC) assembles in non-aqueous electrolyte, and achieves mixed ion- and electronic-conductivity when HBC radical cations are introduced to the assembly (Fig. 1B). Up to 20-fold gains in shuttling current are demonstrated for HBC/HBC$^{\bullet+}$ mixed nanowire assemblies compared to assemblies of undoped HBC. We rationalize this behaviour using density functional theory (DFT), which supports a highly delocalized spin density across the π-conjugated surface of the neutral and oxidized HBCs.

This work suggests new avenues to tailor the properties of multicomponent, electrochemically-active fluids using synthetic chemistry and supramolecular design principles[8] to influence the atomic and electronic structure of the components, the chemical potentials required for doping, and the network's dynamic 3-D architecture across multiple length scales.

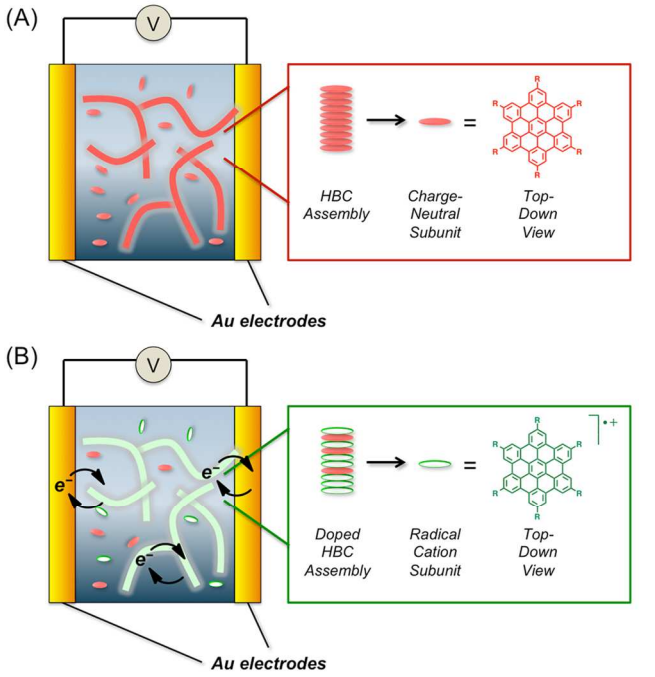

Fig. 1 Schematic representation of HBC assembly into supramolecular networks in liquid electrolyte (A) and subsequent chemical doping by HBC radical cations, which enhance the electronic charge transporting ability of the network (B).

The molecular design of the PAH subunits is based on a HBC platform.[9] Uniquely, *N,N*-dimethylhexanamides are placed at the HBC periphery alongside 2,5-difluorinated benzyls appended to the central coronene. The former confers solubility in a broad range of electrolytes, while the latter was installed to encourage favourable

interactions[10] with endogenous counterions containing fluorine once the HBC subunits are oxidized to radical cations.

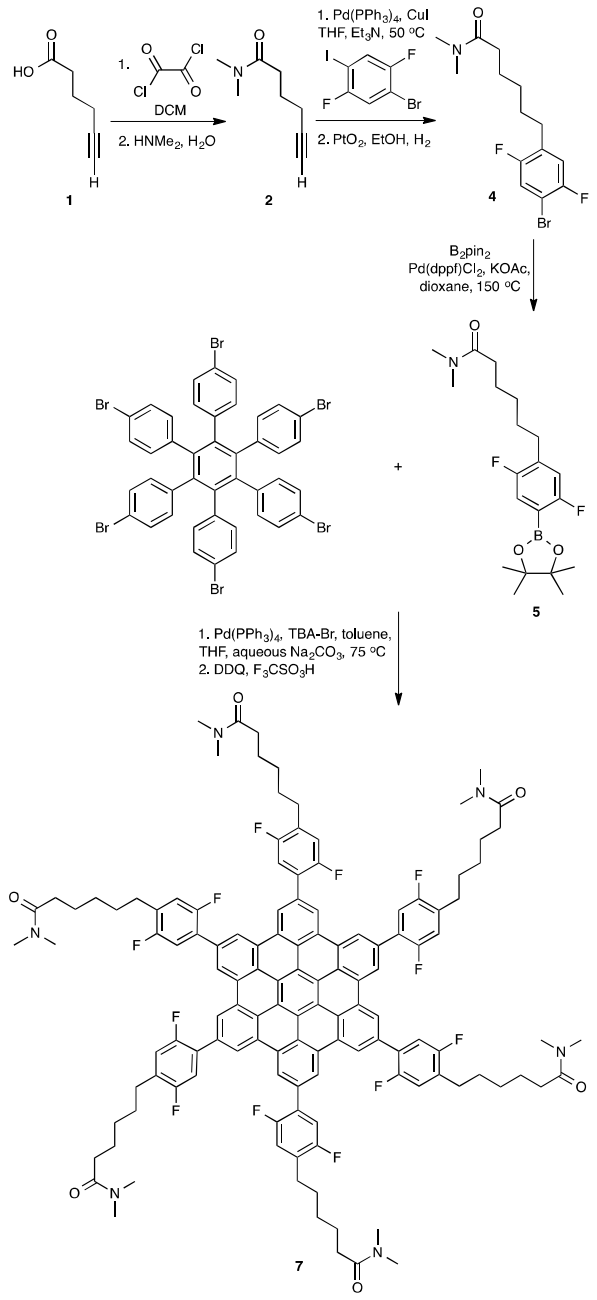

Scheme 1 Chemical synthesis of fluorinated HBC **7**.

The chemical synthesis (Scheme 1) of the HBC subunits was carried out by first treating 5-hexynoic acid (**1**) with oxalyl chloride followed by dimethylamine to access *N,N*-dimethylhex-5-ynamide (**2**) in 88% yield. This intermediate was subjected to a Sonogashira coupling with 1-bromo-2,5-difluoro-4-iodobenzene to yield 6-(4-bromo-2,5-difluorophenyl)-*N,N*-dimethylhex-5-ynamide (**3**), which was then hydrogenated using catalytic amounts of Adam's catalyst (**4** in 87% over two steps). Conversion of aryl bromide **4** to the pinacol boronate ester **5** was carried out with $Pd(dppf)Cl_2$, bis(pinacolato)diboron and KOAc in dioxane at 150 ºC using microwave heating (85%). For the HBC core, hexaphenylbenzene was first brominated[11] using Br_2 prior to Suzuki coupling with **5** under phase transfer conditions using aqueous Na_2CO_3 as the base; to maximize conversion to **6** (52 %), we found a solvent mixture of toluene and THF was required. Finally, a modified Scholl reaction[12] was applied to yield target HBC **7** (25%).

The assembly of **7** into supramolecular polymers and networks was interrogated using UV-Vis-NIR spectroscopy and scanning electron microscopy (SEM) (Figs. 2A–C). Distinctive changes in the optical extinction coefficient (ε) with concentration (*c*) were observed for **7**, consistent with the formation of a π-stacked HBC supramolecular polymer in electrolyte.[13] Increasing *c* from 1.1 μM to 25 μM (benzonitrile, 0.10 M $TBAPF_6$) shows a decrease in ε at all wavelengths, as well as a decrease in fine-structure above 400 nm (Fig 2A). Similar changes are observed for a 10 μM solution (benzonitrile, 0.10 M $TBAPF_6$) when decreasing the temperature from 90 °C to 30 °C (Fig. 2B). The HOMO-LUMO gap calculated from the onset of absorption (1.1 μM HBC **7**, benzonitrile, 0.10 M $TBAPF_6$) is 2.74 eV. A UV-vis spectrum obtained from a film cast from benzonitrile shows in onset of absorption at 2.51 eV (Figure S1). The lower value in the solid state is due to increased excitonic coupling and is indicative of increased assembly of HBC **7** in the solid state.[14] Highly-networked aggregates of **7**, fractal in character, were apparent in the SEM upon drying from salt-free benzonitrile solutions. Nanowires spanning >10 μm were pervasive (Fig. 2C).

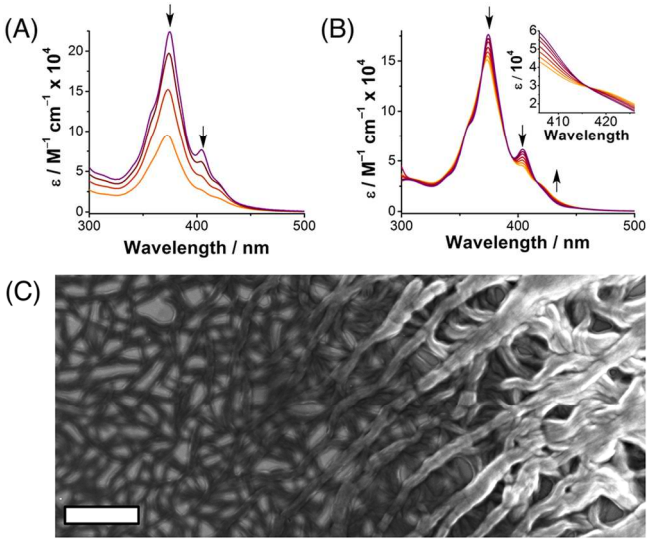

Fig. 2 (A) Variation in the optical extinction coefficient (ε) with concentration (*c*). Arrows indicate change with increasing *c*. (B) Variation in ε with temperature (*T*). Arrows indicate change with decreasing *T* (90 °C to 30 °C). Inset: Isosbestic point at λ = 416 nm (C) SEM of supramolecular networks of HBC **7**. Scale bar = 2 μm.

Assessment of the electronic structure of HBC **7** in the condensed phase was provided by soft X-ray spectroscopy.[15] X-ray absorption (XAS) and X-ray emission (XES) spectra of HBC **7** were evaluated at the carbon K-edge to inform the energy level alignment for the unoccupied and occupied frontier molecular orbitals of the networked HBC, respectively; these orbitals are most closely associated with electronic charge transport (Fig. 3C). The HOMO-LUMO gap was calculated to be 1.96 eV, as determined by

the difference between the highest and lowest energy peak in the first derivative of the XES and XAS spectra, respectively. This value is not comparable to the UV-Vis data because of differing excitonic coupling of core versus valence electronic excitations.

Additional insight into the nature of the molecular orbitals involved in charge transport through π-stacks of HBC **7** was obtained by density functional theory (DFT), where the alkyl side-chains were truncated to methyl groups (see SI). Both the HOMO and LUMO are spread across the PAH π-core of the molecule. Extensive delocalization of the HOMO across the π-system, as is observed in Fig. 3A, helps to stabilize the radical cation as well as facilitates hopping through a network assembled through π-stacking. The calculated spin density of HBC$^{\bullet+}$ **8** also exhibits delocalization over the entire aromatic core.

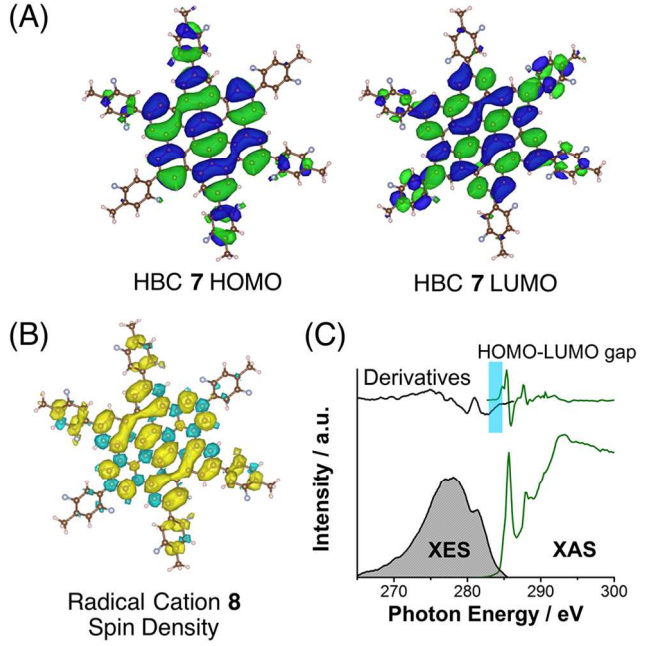

Fig. 3 Calculated representations of (A) frontier molecular orbitals of HBC **7** and (B) spin density of HBC$^{\bullet+}$ **8**. (C) XES and XAS spectra of HBC **7** and their corresponding first derivatives, which quantitatively inform the density of states for the HBC **7** network in the condensed phase.

Chemical doping is essential to enhance charge transport in self-assembled stacks of organic semiconductors; however, the phenomenon is rarely investigated in solution. Therefore, the chemical oxidation of HBC **7** in electrolyte was performed to probe the redox chemistry and transport behaviour of dynamic assemblies of HBC **7**. Tris(4-bromophenyl)ammoniumyl hexachloroantimonate or "Magic Blue" (MB) was a superior oxidizing agent for generating HBC radical cations, owing to the presence of Lewis basic dimethylamides in HBC **7** (which were found to be incompatible with $SbCl_5$ and $NOBF_4$).[15] Electron paramagnetic resonance (EPR) spectroscopy was obtained of an electrolyte solution of HBC **7** after reaction with 0.5 molar equivalents of MB. The EPR spectrum displayed a resonance with a *g* value of 2.0054, confirming that a stable radical (HBC$^{\bullet+}$ **8**) forms at room temperature upon reaction with MB (Fig. S3). Controlled addition of MB to a solution of HBC **7** in electrolyte led to the growth of a peak at λ_{max} = 1025 nm in the optical spectra, consistent with generation of a HBC radical cation (Fig. 4A).[16] The intensity of the peak associated with HBC$^{\bullet+}$ **8** increased until one molar equivalent of MB was added, after which point excess MB was observed (λ_{max} = 721 nm); this supports a quantitative one-electron oxidation. We also showed that the oxidation of HBC **7** to HBC$^{\bullet+}$ **8** is reversible; after addition of excess Zn powder, HBC **7** is observed by optical spectroscopy (Fig. S2).

Self-assembly of HBC **7** in a partially oxidized state was interrogated by variable temperature optical spectroscopy. MB (0.25 eq.) was added to a solution of HBC **7** (10 μM in electrolyte) to form a 3:1 mixture of HBC **7**:HBC$^{\bullet+}$ **8**. Upon heating the solution from 30 to 90 °C changes consistent with a disassembly process are observed: sharpening of the spectral features and increased ε (Fig. 4B). Isosbestic points are observed at 352.5, 358.0, 363.5, and 423 nm, indicating that only the one process is occurring (i.e., disassembly). The temperature induced changes are similar to those observed for neutral HBC **7** alone (Fig. 2B), although the increase in optical density is more extreme for the mixed HBC **7**:HBC$^{\bullet+}$ **8** system and the isosbestic points are shifted slightly.

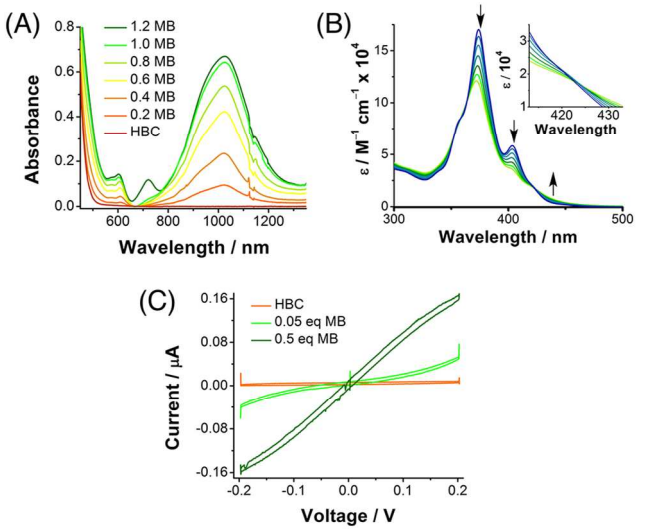

Fig. 4 (A) UV-vis spectroscopy obtained during the chemical oxidation of **7** with controlled amounts of MB in electrolyte. (B) Variable temperature UV-Vis of a 3:1 mixture of **7**:**8** between 30 and 90 °C. Arrows indicate change with decreasing temperature. Inset: Isosbestic point at λ = 423 nm (C) I-V curves of different ratios of **7**:**8.**

By interchanging charge-neutral HBC subunits **7** with radical cation subunits **8** within the assembly, enhanced electronic transport should be possible via hopping.[17,9b] This hypothesis was tested by measuring the shuttling current for HBC assemblies in solution with varying rations of HBC **7**:HBC$^{\bullet+}$ **8**. To evaluate the shuttling current, we carried out *I-V* measurements for electrolyte alone, charge-neutral HBC **7** assemblies, and HBC assemblies doped with controlled amounts of MB (1.25 mM HBC in benzonitrile with 0.10 M $TBAPF_6$). At this concentration HBC **7** should be fully assembled into a supramolecular network; the concentration series (Fig. 2A) showed extensive assembly at 25 μM so we expect complete assembly when 50 times higher. These measurements employed an interdigitated array (IDA) of Au microelectrodes. All IDA measurements were made with one set of electrodes connected to the working electrode lead and the other set connected to the reference and auxiliary leads of the potentiostat. The voltage bias was cycled over a ± 0.2 V range from the open circuit potential (Fig. 4C). Self-assembled networks of charge-neutral HBC **7** show a negligible increase in current over electrolyte. On the other hand, as self-assembled networks of HBC

7 are oxidatively doped by the addition of MB a steady increase in shuttling current is observed up to a maximum current at a 1:1 ratio of HBC **7**:HBC$^{\bullet+}$ **8**. Upon complete oxidation to HBC$^{\bullet+}$ **8**, the shuttling current decreases slightly (Fig. S4). This may be due to disassembly of the charge-transporting nanowires upon further oxidation; electrostatic repulsion between contiguous cation units and increased steric hindrance due to associated counter anions likely promote disassembly of the network upon further oxidation.

These results indicate that HBC **7** is able to transport charge as part of a supramolecular redox-active network in solution. Our work resonates with previous work on the charge-transporting properties of chemically-doped HBC networks in the condensed phase[18,9b] and their application in solid-state electronic devices.[19] Furthering our understanding of their transport behavior in solution is important towards expanding the benefits organic semiconductor materials, such as tunability and processability, to solution-based electrochemical devices.

Conclusions

We have demonstrated that chemical doping enhances electronic charge transport in networks of HBCs assembled in non-aqueous electrolyte. Our results suggest that these networks, and possibly others assembled from different PAHs, are well-positioned to be integrated in electrochemical devices where charge-transport bottlenecks limit device performance. This could include their application as nanostructured redox mediators, given the exceptionally low reorganization energy required for charge transfer to (or from) PAHs across electrolyte-current collector interfaces. Likewise, their use as embedded current collectors may also be feasible, which would allow their use in redox flow batteries; conferring band-like transport throughout the network would significantly enhance their prospects in this regard. Thus, the fundamental science of responsive and reconfigurable supramolecular polymers and networks with tunable charge transport properties is rich with opportunity for both materials chemistry and device physics.

Acknowledgements

This work was supported by the Joint Center for Energy Storage Research, an Energy Innovation Hub funded by the U.S. Department of Energy, Office of Science, Office of Basic Energy Sciences. Portions of the work—including synthesis, structural characterization, and electroanalytical characterization—were carried out as part of a user project at the Molecular Foundry, which is supported by the Office of Science, Office of Basic Energy Sciences, of the U.S. Department of Energy under contract no. DE-AC02-05CH11231. XAS and XES measurements were carried out on BL 8.0.1 at the Advanced Light Source, which is supported by the Director, Office of Science, Office of Basic Energy Sciences, of the U.S. Department of Energy under the same contract. We thank Kevin Wujcik for assistance with EPR spectroscopy.

Notes and references

[a] The Joint Center for Energy Storage Research, Lawrence Berkeley National Laboratory, 1 Cyclotron Road, Berkeley, CA 94720 USA.
[b] The Molecular Foundry, Lawrence Berkeley National Laboratory, 1 Cyclotron Road, Berkeley, CA 94720 USA.
[c] The Advanced Light Source, Lawrence Berkeley National Laboratory, 1 Cyclotron Road, Berkeley, CA 94720 USA.
Electronic Supplementary Information (ESI) available: Synthesis and characterization of all compounds, computational details, experimental details for optical spectroscopy, X-ray spectroscopy, EPR spectroscopy, and electrochemical measurements. See DOI: 10.1039/c000000x/

1 (a) R. H. Friend, R. W. Gymer, A. B. Holmes, J. H. Burroughes, R. N. Marks, C. Taliani, D. D. C. Bradley, D. A. Dos Santos, J. L. Brédas, M. Lögdlund, W. R. Salaneck, *Nature*, 1999, **397**, 121; (b) A. R. Murphy, J. M. J. Fréchet, *Chem. Rev.,* 2007, **107**, 1066; (c) C. Wang; H. Dong, W. Hu, Y. Liu, D. Zhu, *Chem. Rev.*, 2012, **112**, 2208.
2 (a) W. Lu, A. G. Fadeev, B. Qi, E. Smela, B. R. Mattes, J. Ding, G. M. Spinks, J. Mazurkiewicz, D. Zhou, G. G. Wallace, D. R. MacFarlane, S. A. Forsyth, M. Forsyth, *Science*, 2002, **297**, 983; (b) P. M. Beaujuge, J. R. Reynolds, *Chem. Rev.*, 2010, **110**, 268; (c) M. Wu, X. Xiao, N. Vukmirovic, S. Xun, P. K. Das, X. Song, P. Olalde-Velasco, D. Wang, A. Z. Weber, L.-W. Wang, V. S. Battaglia, W. Yang, G. Liu, *J. Am. Chem. Soc.*, 2013, **135**, 12048; (d) W. Li, Q. Zhang, G. Zheng, Z. W. Seh, H. Yao, Y. Cui, *Nano Lett.*, 2013, **13**, 5534; (e) B. Wang, T. J. Richardson, G. Chen, *J. Electrochem. Soc.*, 2014, **161**, A1039; (f) B. Kumar, K. V. Rao, S. Sampath, S. J. George, M Eswaramoorthy, *Angew. Chem. Int. Ed.*, 2014, **53**, 13073; (g) A. S. Weingarten, R. V. Kazantsev, L. C. Palmer, M. McClendon, A. R. Koltonow, A. P. S. Samuel, D. J. Kiebala, M. R. Wasielewski, S. I. Stupp, *Nat. Chem.*, 2014, **6**, 964.
3 (a) M. Duduta, B. Ho, V. C. Wood, P. Limthongkul, V. E. Brunini, W. C. Carter, Y.-M. Chiang, *Adv. Energy Mater.*, 2011, **1**, 511; (b) B. Dunn, H. Kamath, J.-M. Tarascon, *Science*, 2011, **334**, 928; (c) P. Leung, X. Li, C. Ponce de Leon, L. Berlouis, C. T. J. Low, F. C. Walsh, *RSC Adv.*, 2012, **2**, 10125; (d) Q. Huang, Q., Wang, *ChemPlusChem*, 2015, **80**, 312.
4 T. Fukushima, A. Kosaka, Y. Ishimura, T. Yamamoto, T. Takigawa, N. Ishii, T. Aida, *Science* 2003, **300**, 2072; (b) J. Lee, T. Aida, *Chem. Commun.*, 2011, **47**, 6757; (c) F. Y. Fan, W. H. Woodford, Z. Li, N. Baram, K. C. Smith, A. Helal, G. H. McKinley, W. C. Carter, Y.-M. Chiang, *Nano Lett.*, 2014, **14**, 2210.
5 (a) E. Papirer, R. Lacroix, J. B. Donnet, *Carbon* 1996, **34**, 1521. (b) D. Tasis, N. Tagmatarchis, A. Bianco, M. Prato, *Chem. Rev.*, 2006, **106**, 1105; (c) V. Georgakilas, M. Otyepka, A. B. Bourlinos, V. Chandra, N. Kim, K. C. Kemp, P. Hobza, R. Zboril, K. S. Kim, *Chem. Rev.*, 2012, **112**, 6156.
6 (a) J. Wu, W. Pisula, K. Müllen, *Chem. Rev.*, 2007, **107**, 718; (b) L. Zang, Y. Che, J. S. Moore, *Acc. Chem. Res.*, 2008, **41**, 1596; (c) C. Huang, S. Barlow, S. R. Marder, *J. Org. Chem.*, 2011, **76**, 2386.
7 V. Coropceanu, J. Cornil, D. A. da Silva Filho, Y. Olivier, R. Silbey, J.-L. Brédas, *Chem. Rev.*, 2007, **107**, 926.
8 (a) L. Brunsveld, B. J. B. Folmer, E. W. Meijer, R. P. Sijbesma, *Chem. Rev.*, 2001, **101**, 4071; (b) T. Aida, E. W. Meijer, S. I. Stupp, *Science*, 2012, **335**, 813.
9 (a) A. M. van de Craats, J. M. Warman, A. Fechtenkotter, J. D. Brand, M. A. Harbison, K. Müllen, *Adv. Mater.*,1999, **11**, 1469. (b) J. P. Hill, W. Jin, K. Kosaka, T. Fukushima, H. Ichihara, T. Shimomura, K. Ito, T. Hashizume, N. Ishii, T. Aida, *Science*, 2004, **304**, 1481.
10 F. T. T. Huque, K. Jones, R. A. Saunders, J. A. Platts, *J. Fluor. Chem.*, 2002, **115**, 119.
11 R. Rathore, C. L. Burns, *Org. Syn.*, 2005, **82**, 30.
12 D. J. Jones, B. Purushothaman, S. Ji, A. B. Holmes, W. W. H. Wong, *Chem. Commun.*, 2012, **48**, 8066.

13 (a) X. Dou, W. Pisula, J. Wu, G. J. Bodwell, K. Müllen, *Chem. Eur. J.* 2008, **14**, 240; (b) X. Feng, W. Pisula, T. Kudernac, D. Wu, L. Zhi, S. De Feyter, K. Müllen, *J. Am. Chem. Soc.*, 2009, **131**, 4439.
14 J.-L. Bredas, *Mater. Horiz.*, 2014, **1**, 17.
15 (a) M. Keil, P. Samori, D. A. dos Santos, T. Kugler, S. Stafström, J. D. Brand, K. Müllen, J. L. Brédas, J. P. Rabe, W. R. Salaneck, *J. Phys. Chem. B*, 2000, **104**, 3967; (b) H. Glowatzki, G. N. Gavrila, S. Seifert, R. L. Johnson, J. Räder, K. Müllen, D. R. T. Zahn, J. P. Rabe, N. Koch, *J. Phys.Chem. C*, 2008, **112**, 1570.
16 R. Rathore, C. L. Burns, *J. Org. Chem.*, 2003, **68**, 4071.
17 L. Chen, K. S. Mali, S. R. Puniredd, M. Baumgarten, K. Parvez, W. Pisula, S. de Feyter, K. Müllen, *J. Am. Chem. Soc.*, 2013, **135**, 13531.
18 (a) Q. Zhang, P. Prins, S. C. Jones, S. Barlow, T. Kondo, Z. An, L. D. A. Siebbeles, S. R. Marder, *Org. Lett.*, 2005, **7**, 5019. (b) A. M. van de Craats, J. M. Warman, A. Fechtenkötter, J. D. Brand, M. A. Harbison, K. Müllen, *Adv. Mater.*, 1999, **11**, 1469.
19 (a) E.-K. Fleischmann, R. Zentel, *Angew. Chem. Int. Ed.*, 2013, **52**, 8810. (b) W. W. H. Wong, T. B. Singh, D. Vak, W. Pisula, C. Yan, X. Feng, E. L. Williams, K. L. Chan, Q. Mao, D. J. Jones, C.-Q. Ma, K. Müllen, P. Bäuerle, A. B. Holmes, *Adv. Funct. Mater.*, 2010, **20**, 927. (c) L. Schmidt-Mende, A. Fechtenkötter, K. Müllen, E. Moons, R. H. Friend, J. D. MacKenzie, *Science*, 2001, **293**, 1119.

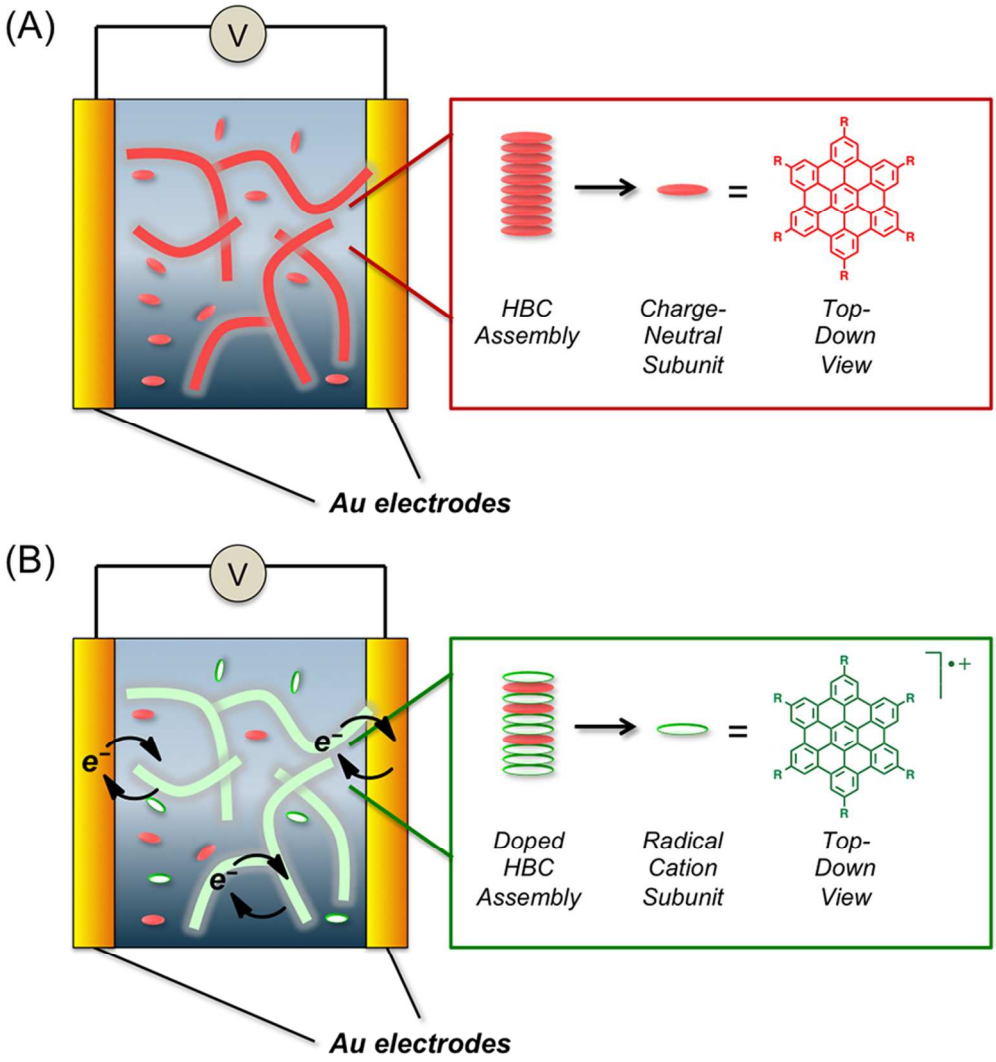

83x89mm (300 x 300 DPI)

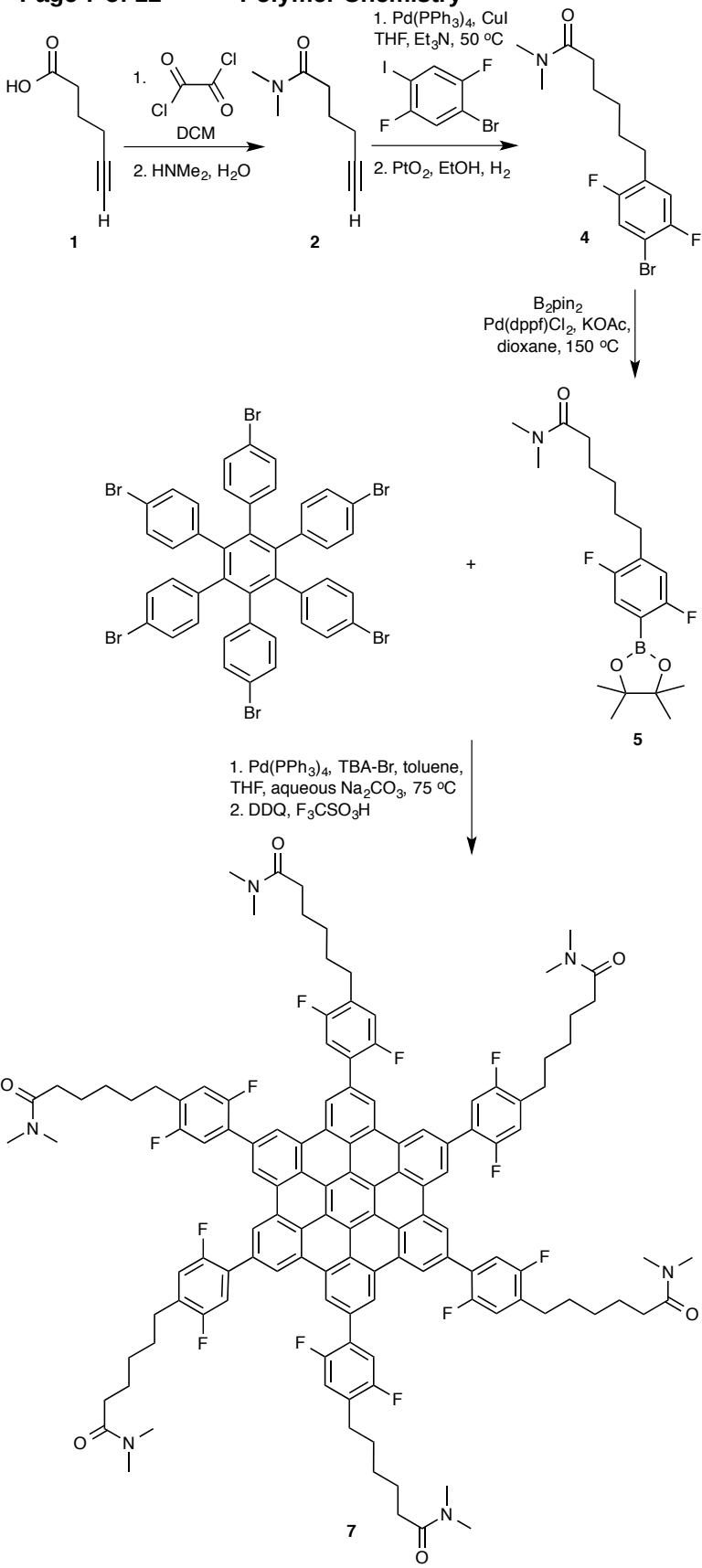
1. Pd(PPh3)4, CuI
THF, Et3N, 50 °C
1.
DCM
2. HNMe2, H2O
2. PtO2, EtOH, H2
1
2
4
B2pin2
Pd(dppf)Cl2, KOAc,
dioxane, 150 °C
5
1. Pd(PPh3)4, TBA-Br, toluene,
THF, aqueous Na2CO3, 75 °C
2. DDQ, F3CSO3H
7

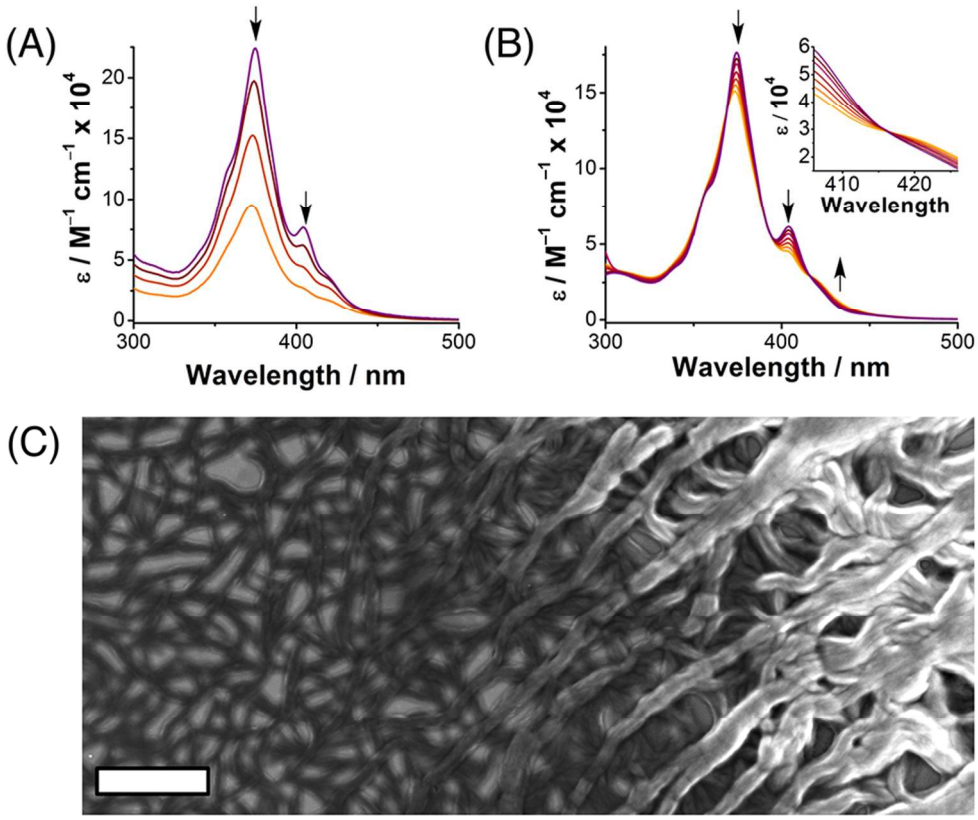

83x68mm (300 x 300 DPI)

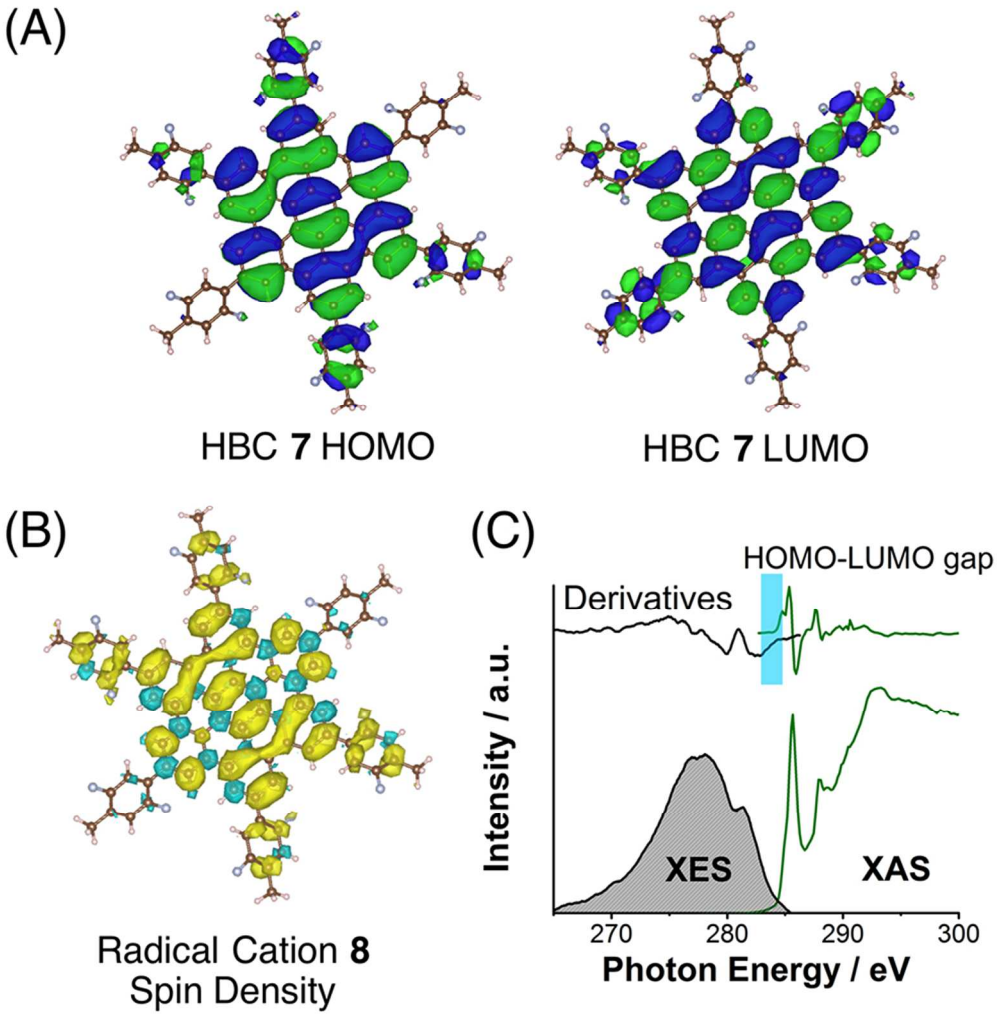

83x85mm (300 x 300 DPI)

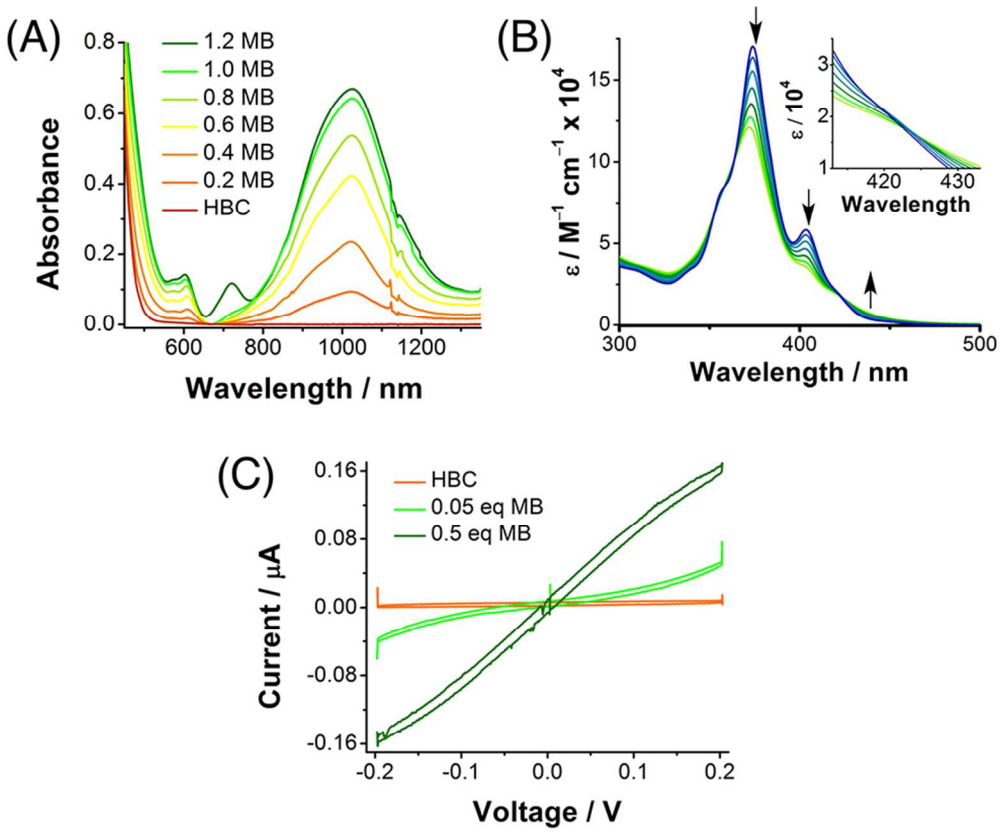

83x70mm (300 x 300 DPI)

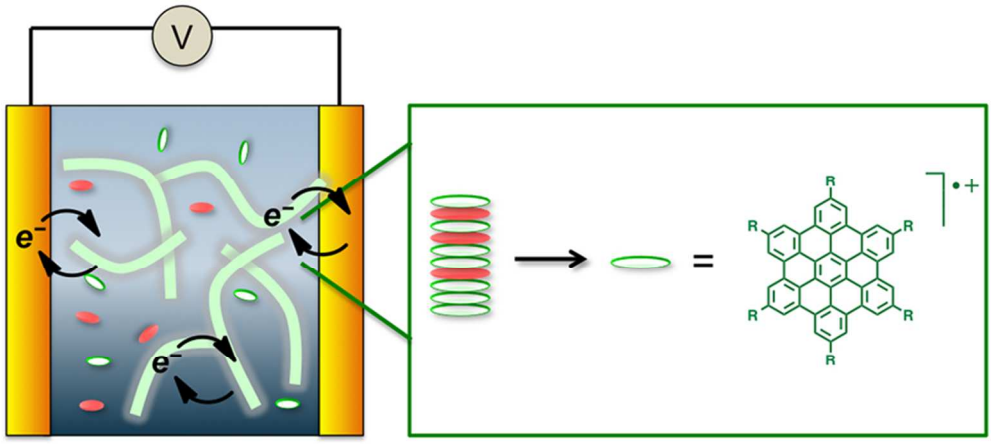

76x34mm (300 x 300 DPI)

The electronic transport properties of HBC networks in non-aqueous electrolyte are tailored using synthetic chemistry and supramolecular design principles.